Front. Phys. 13(1), 138202 (2018)
https://doi.org/10.1007/s11467-017-0686-6

REVIEW ARTICLE

NMR investigation of degradation processes of ancient and modern paper at different hydration levels

Domenico Mallamace[1,†], **Sebastiano Vasi**[2], **Mauro Missori**[3],
Francesco Mallamace[2,4,5], **Carmelo Corsaro**[2,4]

[1] *Consorzio interuniversitario per lo sviluppo dei Sistemi a Grande Interfase - CSGI,*
Via della Lastruccia 3, 50019 Sesto Fiorentino, Firenze, Italy
[2] *Dipartimento MIFT, Sezione di Fisica, Università di Messina,*
Viale F. Stagno D'Alcontres 31, 98166 Messina, Italy
[3] *Istituto dei Sistemi Complessi, Consiglio Nazionale delle Ricerche, Unit Sapienza,*
Piazzale Aldo Moro 5, 00185 Roma, Italy
[4] *CNR-IPCF Messina, Istituto per i Processi Chimico-Fisici, Viale F. Stagno D'Alcontres 37, 98158 Messina, Italy*
[5] *Center for Polymer Studies and Department of Physics, Boston University, Boston, MA 02215, USA*
Corresponding author. E-mail: †*mallamaced@unime.it*

Received February 24, 2017; accepted April 13, 2017

The degradation process of cellulose-made materials was investigated by means of nuclear magnetic resonance (NMR) spectroscopy, with particular emphasis on the role of water and on the hydration mechanism of cellulose fibrils. To accomplish this, the structure and dynamics of water within ancient and modern samples with different aging histories were investigated. The results mainly indicated that hydrolytic and oxidative reactions provoked the formation of acidic by-products. Furthermore, degradation processes were enhanced by higher amounts of water giving a progressive consumption of the amorphous regions of the cellulose. We propose NMR experiments as a benchmark for characterization of the degradation state of paper, as well as for investigating the effectiveness of restoration treatments.

Keywords ancient paper, degradation, NMR, hydration, solvent dynamics

PACS numbers 82.30.Rs, 82.30.Lp, 82.56.Dj, 82.56.-b

Contents

1 Introduction

Hydration water plays a very important role in triggering the biological functioning and chemophysical properties of any biosystem, including proteins, DNA, RNA, etc. [1, 2]. It is noteworthy that the network of hydrogen bonds (HB) formed by water is primarily responsible for inducing the proper flexibility of amino acids, flexibility that is necessary to activate the precise biological function of macromolecules [3, 4]. One of the most ubiquitous biopolymers whose properties are strongly triggered by the presence and amount of water is cellulose. Cellulose is an organic compound consisting of a linear homopolymer composed of β-D-glucopyranose units $(C_6H_{10}O_5)_n$ linked with β-(1→4)-glycosidic bonds to form chains with n values from $\approx 10^2$ to $\approx 10^4$ elements [5]. These chains have a strong inclination to aggregate into highly ordered structures as a consequence of the development of an extended network of both intramolecular and intermolecular hydrogen bonds [5, 6]. Indeed, a hierarchical arrangement is formed, beginning with elemental fibrils (or microfibrils) that are the basic elements of supramolecular structures up to fibers whose diameters range from

---

*Special Topic: Water and Water Systems (Eds. F. Mallamace, R. Car, and Limei Xu).

~ 1 to ~ 10 μm. These microfibrils comprise an assembly of highly ordered (crystalline) domains and of disordered (amorphous-like) regions [5]. The relative amount of polymer within the crystalline domains covers a wide range and depends on the origin and pretreatment of the sample; for native cotton, the amount of cellulose is 60–70% [5, 6]. Recently, smart materials constructed with nanocrystalline cellulose have been proposed for several applications [7, 8].

A system of pores and voids of non-uniform sizes and shapes complement the molecular architecture of cellulose fibers. Some of these pores and voids are confined within the cellulose fibers. Quantitative analysis of the pore-size distribution has shown that the pore diameters range from approximately 1 nm when they are fully confined in the amorphous regions to hundreds of nanometers within the cellulose fibers. The distribution of pores and voids strongly influences the mechanical properties of the cellulose fibers and indeed the reactivity of the cellulose itself as a result of water and external agent accessibility [9–13].

Cellulose is mainly used to produce paper, which is probably the most common and widespread material. In fact, since ancient times, paper has been used as a favorable medium to acquire and store human knowledge [5]. For this reason, paper is also one of the oldest and most precious man-made materials. Paper was invented in China in the 2nd century A.D. and independently in Mesoamerica in the 7th century A.D. From the Far East to the western world in the Middle Ages and for centuries afterward, a growing number of cultural resources have been accumulating in archives, libraries, and museums all over the world [14, 15].

Paper originates from a dilute suspension of cellulose fibers and water in almost equimolar amounts [16, 17] plus small quantities of organic or inorganic additives or impurities [18, 19]. Cellulose is then drained through a sieve, pressed, and dried to remove excess water and attain a sheet composed of a network of randomly interwoven fibers. The paper composition varies depending on the production period and technology employed. Under ambient conditions, approximately 20°C, and 50% relative humidity (RH), paper contains from 5 to 8% water by weight. By soft drying, it is possible to "extract" up to approximately 2% of the water molecules. In fact, a minimal amount of water is part of the paper structure itself by bridging different cellulose chains [12]. This also happens in other biological samples such as proteins, where there is always some amount of water (internal or bound water) that constitutes a structural part of the system and cannot be removed by "soft" heating. In fact, water assumes an essential role in the chemical reactivity and physical properties of paper. In particular, it permits the availability of free protons for the hydrolysis of glycosidic bonds, and molecular oxygen which is a very good vehicle for oxidizing cellulose through the production of active oxygen species (superoxide, hydrogen peroxide, and hydroxyl radicals) [12, 20]. Paper is quite hydrophilic and, under normal ambient conditions, water is sorbed to paper, constituting a significant weight fraction. This phenomenon is called hydration.

The sorption of water is very important for determining the mechanical properties of the cellulose structure. Indeed, at the molecular level, water–cellulose interactions must involve hydrogen bonding with cellulose hydroxyl groups. Furthermore, the power of water to break up hydrogen bonding and the prevalence of polysaccharide chemistry in these materials define the structuring of the local water environments.

From a macroscopic point of view, paper degradation is manifested as a decrease in the intensity of the mechanical properties of the sheets and is associated with widespread or localized yellowing and/or discoloration of the paper. On the microscopic scale, these phenomena are provoked by the acid hydrolysis of β-D-(1,4)-glycosidic bonds and oxidation of the β-D-glucopyranose units of cellulose polymers [5, 14, 20, 21]. Acid hydrolysis, more profound in modern papers , affects the mechanical properties of paper sheets because it reduces the cellulose chains. The breaking of glycosidic bonds is catalyzed either by hydronium cations (H_3O^+) formed through the acidic hydrolysis of internal components such as alum or by the action of cellulolytic enzymes [5]. In contrast to acid hydrolysis, oxidation of cellulose usually starts with the conversion of individual β-D-glucopyranose units to fairly unstable oxidized derivatives, which induces ring opening and/or chain cleavage [5], as well as depolymerization [22, 23]. As a consequence of hydrolysis of glycosidic bonds, depolymerization can be increased significantly by using acidic oxidation products such as carboxylic groups fitted in the cellulose polymer and also by using light products of the degradation such as volatile compounds [24]. In general, these degradation processes finally result in the formation of a great number of low-molecular-mass products such as glucopyranose or other organic compounds such as acetic and formic acids [25].

One of the principal difficulties in the study of the degradation of ancient artifacts is that the environmental conditions to which the samples were subjected throughout their history are unknown. However, artificial and controlled high-temperature aging allows continuous monitoring of the changing environmental conditions, providing useful information for ancient paper conservation [21].

The characterization of light by-products (degradation markers) can be used to estimate paper degradation to obtain useful information about the preservation and conservation of cellulosic materials [24, 26]. The light by-products of paper degradation are usually incremented by increasing the amount of water. Thus, the study of the dynamics of water as a function of the moisture content for artificially aged paper is also important. Usually, three types of water can be identified within cellulosic materials: free water, bound freezing water, and bound non-freezing water [27]. Free water is also known as "easy-to-remove" water, whereas water that is confined in the fiber network and all bound water are classified as "hard-to-remove" water because they are closely bonded to the cellulose hydroxyl groups. All these situations can be investigated by means of different experimental methods such as X-ray and neutron scattering [9, 10], gas or liquid chromatography [24], electrophoresis [25], mass spectrometry [25], theoretical [28] and experimental optical spectroscopy [29–31], and nuclear magnetic resonance (NMR) [32].

Among them, NMR is very sensitive to the different environments experienced by the resonant nuclei and it can discriminate between the same nuclei in different chemical environments [33]. Several NMR approaches have been applied in the past to study paper and cellulose-based materials [17, 18]. However, because of strong dipolar couplings, high resolution (HR) is easily achievable only in solution; to overcome this difficulty, different approaches have been developed to resolve peaks in semi-solid compounds such as soft matter (polymers, polyelectrolytes, gels, etc.), biological samples (cells, DNA, proteins, etc.), intact tissues, organs, food specimens, membranes, and interfaces at or out of equilibrium. One of the most-used experimental techniques is known as ^{1}H high-resolution magic angle spinning (HR-MAS). This technique has been receiving much attention and development because of its powerful versatility in different fields, particularly in medicine, biology, and food science [34–38]. In fact, it permits investigation of microquantities of semi-solid compounds without the need for time-consuming separation procedures, and it is possible to obtain different and detailed information (both structural and dynamical) on all the components of the studied specimen. Indeed, the HR-MAS technique allows researchers to investigate the microscopic details of cellulosic materials and their interaction with water.

In this paper, we report HR-MAS NMR studies on the degradation processes of ancient and modern paper at different hydration levels. In particular, we analyzed the metabolic profiles of the investigated systems by performing peak assignment of the spectra belonging to both ancient and modern papers. Furthermore, we investigated the dynamics of water molecules to shed light on the mechanisms of the interaction between water and cellulose on a nanoscale by measuring the relaxation times and by performing lineshape analysis of the NMR spectra. These kinds of studies are very important for examining the swelling of the cellulose fibers and the acceleration of degradation reactions with the consequent consumption of the amorphous regions.

2 Experiments

All NMR measurements were performed using a Bruker Avance spectrometer operating at 700 MHz (proton Larmor frequency) using the HR-MAS technique [14, 39, 40]. The HR-MAS technique was developed to reduce the two main line-broadening mechanisms, namely, dipolar coupling and heterogeneous isotropic susceptibility [41–43]. These two processes generate a local magnetic field that changes from position to position, corresponding to the changes in the resonance frequency. This causes a frequency distribution for each resonance frequency that depends on the intensity of the two effects. To bypass and reduce these mechanisms, in the HR-MAS technique, the sample is put in a rotor and spun at a magic angle of approximately 54.74° at a few thousands of hertz. Nowadays, the MAS rotor can be spun at frequencies between approximately 1 and 100 kHz; at higher frequencies, the NMR bands are enhanced and show higher resolution.

We used both modern and ancient samples for our experiments. The ancient samples were produced in the 15th century in European countries and they carried no printing. As was the custom in ancient times, the samples were made of cotton and linen cellulose fibers. Two ancient samples, both made in Perpignan, France, in 1413, were labeled A1 and B1, and they were in good and intermediate conservation condition, respectively. A third sample, made in Milan, Italy, in 1430 and labeled A3, was in bad conservation condition (within a water stain). The modern paper samples (labeled P2), provided by the Netherlands Organization for Applied Scientific Research (TNO), were made of unbleached cotton linters. They contained very low amounts of inorganic ingredients (ash content, 0.005% in weight) and no additives or lignin, with a high mean degree of polymerization. The P2 samples were artificially aged in air in a climatic chamber at relative humidity of 59% and a temperature of 90°C for different numbers of days. At 90°C, moderate degradation of the cellulose polymers was expected to occur [22]. The sample labeled P2REF was the non-aged sample. The aged samples were denoted as P2C90xx, where xx represents the number of aging days.

In our work, the metabolic study of these samples was performed by putting 30 μL of D_2O in the rotor with the investigated sample [14]. Individual metabolites were identified by using bi-dimensional homonuclear pulse sequences and by examining the NMR spectra with the aid of NMR Suite Professional version 7.1 (Chenomx, Alberta, Canada) and comparing our results with those found in the literature and in Internet databases (e.g., Human Metabolome Database, www.hmdb.ca). Structural and dynamical measurements were performed using paper samples with different values of moisture content [39, 40]. The moisture content, also called the hydration level, h, is defined as

$$h = \frac{m_{\mathrm{H_2O}}}{m_{dry\ paper}}, \tag{1}$$

where $m_{\mathrm{H_2O}}$ is the mass of water and $m_{dry\ paper}$ is the mass of the completely dry sample. Note that $m_{\mathrm{H_2O}}$ is obtained as the difference between the total sample weight and the value of $m_{dry\ paper}$ estimated by the NMR spectra [39]. We used moisture content values of approximately 2%, 8%, 14%, 20%, and 40%. The samples were initially kept in an oven at 105°C for 4 h to reach a hydration level of approximately 2% that we labeled as "quasi-dry". Then, the dry samples were hydrated in a closed chamber at RH = 100% until reaching the desired moisture content, which was evaluated by weighing the samples before and after each measurement and verifying that the weight remained stable within 5% [39, 40]. The experimental details concerning the acquisition parameters and pulse sequences used in this study are reported elsewhere [14, 39].

3 Results and discussion

Figure 1 shows the ^{1}H HR-MAS NMR spectra of D_2O-hydrated samples (model samples P2REF and P2C9048 and ancient sample A1) from which we were able to classify the main degradation products of the paper.

In the ancient paper, we identified a quite interesting bio-marker in the form of choline and other amino compounds (as well as phenylalanine) that give evidence of ancient production methods [14, 15, 19].

The spectrum of the non-aged model paper sample P2REF (black line in Fig. 1), made of very pure cotton cellulose, showed only two "primary" broad bands, one centered at 1.30 ppm and a much broader one at 1.54 ppm. Secondary bands at 0.86 and a smoother one at approximately 2.16 ppm were also observed, and all belong to different carboxylic acids. The characteristic bands of these acids were more intense than those of cellobiose (3–4.5 ppm), the monomer unit of cellulose [14]. This is due to the higher sensitivity of ^{1}H HR-MAS NMR to amorphous regions than to crystalline regions of cellulose that prevailed in the samples. Degradation processes take place within amorphous regions, and thus the HR-MAS technique was incredibly useful in recognizing degradation products in the ancient samples.

Upon artificial aging of the P2 samples, as the cellulose structure swelled, making the cellulose fibers more accessible to water and oxygen, the increased molecular mobility resulted in new features in the ^{1}H NMR spectra. In the spectrum of the most artificially aged P2C9048 sample (Fig. 1, dark yellow line), sharp peak components increased whereas the broad resonances decreased. This tendency is probably related to the fact that paper was hydrated during the aging process, thus showing signals of mobile cellulose-like species (3–4 ppm) and light by-products of cellulose degradation (0–3 ppm) (see Ref. [14] for more details).

All compounds detected in the modern artificially aged samples were also found in the ancient paper sample A1 (Fig. 1 green line), although the bands assigned to them showed slightly different shapes and intensities. The ^{1}H NMR spectrum of ancient sample A1 was characterized by a flat background similar to that observed for the most degraded modern sample, P2C9048. This confirms that degradation processes affect amorphous regions, which

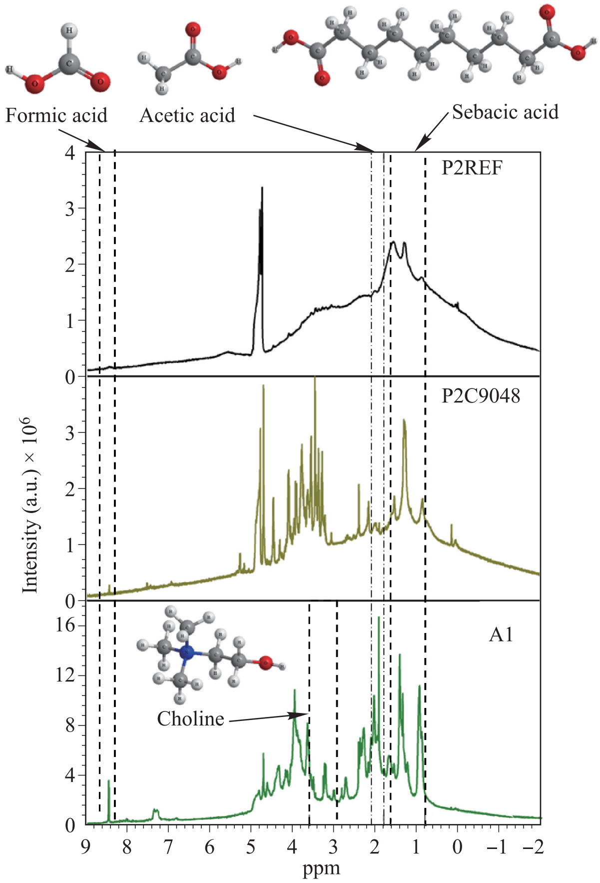

Fig. 1 ^{1}H HR-MAS NMR spectrum of non-aged sample P2REF (top panel, *black line*), P2C9048 (middle panel, *light green line*), and ancient sample A1 (bottom panel, *dark green line*). The chemical structures of some degradation products of cellulose are also shown.

become disrupted and then more mobile, thus providing well-resolved sharp peaks in the ^{1}H NMR spectra. This can also be inferred from the sharpening of the peak centered at approximately 1.99 ppm.

Concerning samples with different hydration levels, we performed lineshape analysis of the NMR signal [40]. Figure 2 shows the best fit obtained for the MAS NMR spectra of the hydrated P2REF sample with the pseudo-Voigt function described by

$$y = A\left[\mu\frac{2}{\pi}\frac{\omega_L}{4\left(x-x_c\right)^2+w_L^2} +(1-\mu)\frac{\sqrt{4\ln 2}}{\sqrt{\pi}w_G}\mathrm{e}^{-\frac{4\ln 2}{w_G^2}(x-x_c)^2}\right], \tag{2}$$

where A is the amplitude, μ is the weight of the two components, x_c is the peak position, and w_L and w_G are the widths of the Lorentzian and Gaussian contributions of water and cellulose protons, respectively [16, 44, 45]. The four panels show the four different hydration levels considered for that sample. The total fit with the pseudo-Voigt function is shown as a red line and the two contributions as a green line (Lorentzian) and a blue line (Gaussian). Note that the Gaussian function gives essentially the same contribution as the Lorentzian one only for the sample with the lowest hydration ($\mu = 0.63$), turning into a negligible background at higher h values ($\mu = 0.94$ for $h = 41\%$).

For water systems, the proton chemical shift reproduces the local arrangement of the local hydrogen bond (HB) geometry [40, 46, 47]. Consequently, a study of the trend of the measured peak position (x_c) versus the hydration level allowed detailed analysis of the evolution of the water local structure in terms of HB formation [48, 49]. Another important parameter is the width of the Lorentzian function, ω_L, because it describes the interaction between water molecules, and so accounts for the formation of ordered hydrogen-bonded structures which is progressively prevented by the increased presence of degradation by-products in the hydrated paper. We focused our attention on the dependence of ω_L on h that shows a decreasing trend with increasing hydration, as shown in Fig. 2. The last parameter we obtained by the analysis of the NMR spectra was the area of the Lorenztian function obtained by multiplying the parameters A and μ of Eq. (2) ($A_L = A \cdot \mu$). Figure 3 shows all the abovementioned parameters of the pseudo-Voigt expressed by Eq. (2) as a function of hydration for three studied samples: P2REF (not aged, black squares), P2C9048 (artificially aged, red circles), and A1 (ancient

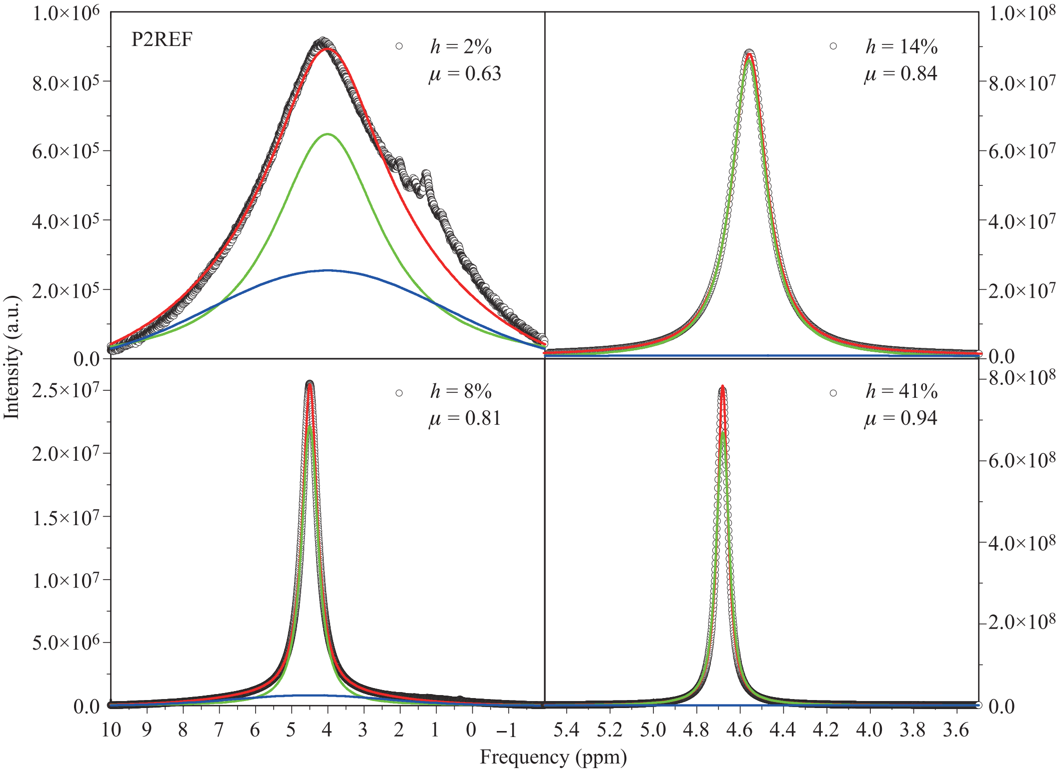

Fig. 2 The proton HR-MAS NMR spectra of P2REF samples at different hydration levels. We use two x-axes for the left and right sides and every panel has a different intensity scale. The total fit with the pseudo-Voigt function (*red line*) and the two components, Lorentzian (*green line*) and Gaussian (*blue line*), are reported.

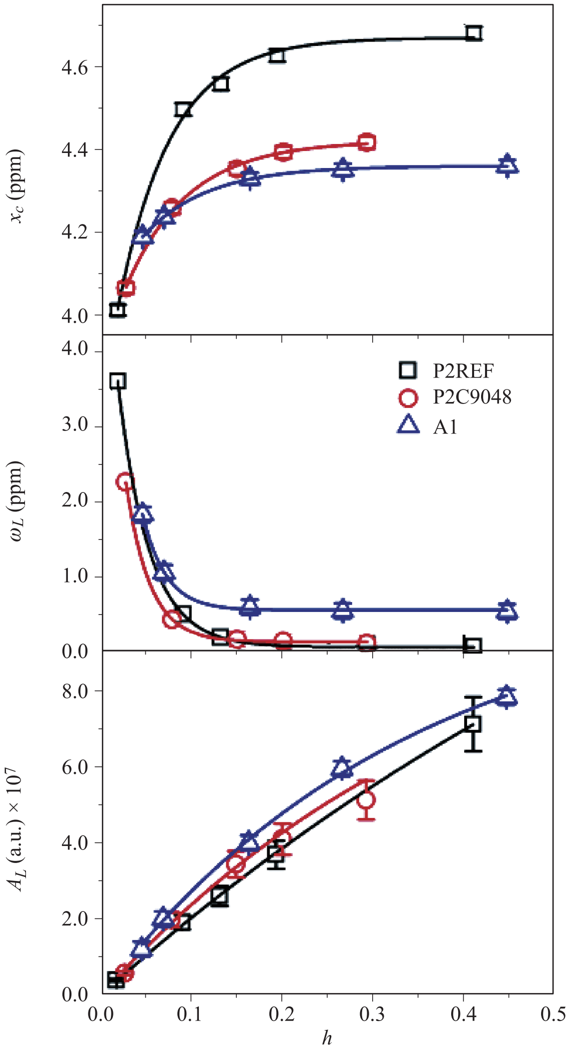

$x_c\,(h) = (x_0 - x_f)\,\mathrm{e}^{-h/h_x} + x_f$

	x_f (ppm)	h_x	x_0 (ppm)
□ P2REF	4.67±0.02	0.059±0.006	3.80±0.04
○ P2C9048	4.42±0.01	0.069±0.005	3.91±0.02
△ A1	4.36±0.01	0.071±0.003	4.04±0.01

$\omega_L\,(h) = (\omega_0 - \omega_f)\,\mathrm{e}^{-h/h_\omega} + \omega_f$

	ω_f (ppm)	h_ω	ω_0 (ppm)
□ P2REF	0.058±0.001	0.034±0.001	5.793±0.002
○ P2C9048	0.13±0.01	0.026±0.001	5.8±0.2
△ A1	0.55±0.01	0.025±0.001	7.7±0.7

$A_L\,(h) = A_f\,(1 - \mathrm{e}^{-h/h_A})$

	A_f (a.u. × 10^8)	h_A
□ P2REF	1.9±0.1	0.9±0.1
○ P2C9048	1.1±0.2	0.4±0.1
△ A1	1.08±0.05	0.34±0.03

Fig. 3 The evolution of the three parameters, x_c, ω_L, and A_L, in the pseudo-Voigt function [Eq. (2)]. Black squares, red circles, and blue triangles correspond to P2REF, P2C9048, and A1 samples, respectively. Lines are best-fit and the corresponding obtained parameters are reported in the tables. Figure adapted from Ref. [40].

paper, blue triangles). The behavior of x_c is exponential-like, and it can be modeled by the functions reported in Fig. 3 at the right side of the top panel, together with the values of the three parameters in a table obtained by a best-fit procedure (solid lines). In this case, the increasing degradation provoked a slower hydration process; in fact, the increasing oxidation of the cellulose polymers (as degradation proceeded) promoted the repulsion of new additional water molecules by means of hydrophobic interactions [39].

The middle panel of Fig. 3 shows that the dependence of ω_L on the hydration can be described by the same exponential function used to perform the best fit of the x_c data rewritten in terms of ω_L.

Concerning $A_L(h)$, even in this case, its behavior can be well fitted by an exponential function where, of course, its value must be zero for the totally dry sample. Note that the behavior of $A_L(h)$ is almost linear for P2REF. This is an indication that the non-aged sample weakly influenced the water behavior being an almost inert host. On the other hand, for the aged samples, the amphiphilic character of the different by-products and cellulose surfaces determined the complex dependence on hydration.

Regarding the dynamical analysis, we studied the NMR relaxation times T_1 and T_2 [39]. Here, we show the behavior of the longitudinal relaxation time T_1 as a function of the hydration level and of the number of degradation days. Note that T_1 gives an estimation of the interaction strength, and it represents the correlation between the system–environment energy exchange and the stiffness of the bonds.

A faster energy exchange between the observed spin system and the surrounding environment provokes a lowering of T_1, and thus it corresponds to stronger interactions [50]. We found that T_1 consisted of three different components (denoted as T_{1a}, T_{1b}, and T_{1c}), which showed different behaviors as a function of moisture content or the hydration of the cellulose [39]. Figure 4 (left) shows the P2REF and P2C9048 data for each component. The T_{1a} component is the slowest one, and it has exponential-like behavior as a function of h. We attributed this to free water. Note that for the smallest hydration, T_{1a} shows the longest value in respect to that of bulk water, which shows a T_1 value of 3 s at ambient temperature [51, 52]. T_{1b} is attributed to non-freezing water that cannot be removed. This component has a constant trend as a function of h because non-freezing water steadily interacts with the hydroxyl groups of cellulose. Finally, the T_{1c} component has the smallest value, which slowly increases with increasing h. We attribute this relaxation time to that of cellulose protons, in agreement with Refs. [16, 51, 53, 54].

We also evaluated T_1 as a function of the number of degradation days, including the three naturally aged samples (denoted as A1, B1, and A3) by means of HR-MAS NMR [39].

Figure 4 (right) shows the trend of the three different contributions of T_1 mentioned above as a function of the number degradation days [39]. T_{1a} increases its value from that of P2REF to that of P2C9012, and then it decreases linearly with the increasing number of degradation days. This is why the first step of the degradation process provokes the rupture of intramolecular HBs. After 12 degradation days under the considered conditions, the hydroxyls were progressively oxidized into carbonyls. This transformation was particularly perceptible for the ancient samples, where T_{1a} sharply decreased as a function of the degradation. Note that the T_{1a} values for the ancient samples (blue squares in Fig. 4) were placed on the extrapolation of the linear fit performed for the aligned values of the modern samples artificially aged for more than 12 days. In such a way, we estimated the corresponding equivalent artificial degradation days: 157, 170, and 189 for A1, B1, and A3, respectively. It was surprising that there was a fine consistency among the values of the other two components, which followed a linear evolution starting from the values of the modern samples. Furthermore, these three linear trends cross each other with very good approximation at approximately 212 degradation days. Indeed, this should mark the limit of artificial degradation, at which point the paper loses most of its mechanical properties and starts to crumble. In fact, the mechanical characteristics of paper sheets are lowered by processes such as acidic hydrolysis [55]. The degradation processes are linked with a decreasing number of interchain water molecules (bound water) whose hydrogen bonds are broken by the presence of the solvent molecules (free water). Note that Fig. 4 (right) provides an explanation of the comparable values of all T_1 components for the P2REF and P2C9048 samples as a function of hydration shown in Fig. 4 (left). This strict similarity can be clarified by the first increase with degradation of the solvent-accessible regions later compensated by the oxidation of hydroxyl groups.

We also measured the transverse relaxation time T_2

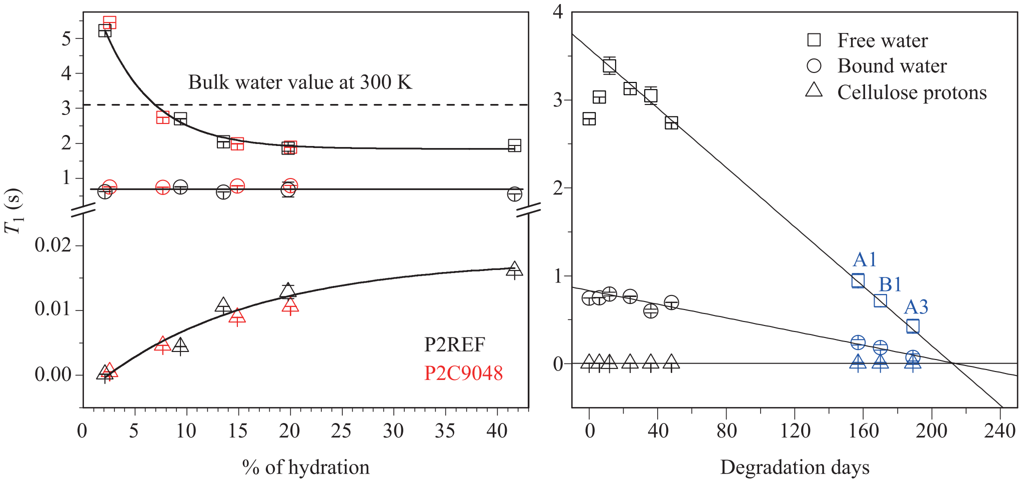

Fig. 4 Left panel: T_1 data of the three different contributions as a function of the hydration for both P2REF (*red symbols*) and P2C9048 (*black symbols*) samples. The lines are visual guides. Right panel: T_1 data of the three contributions as a function of the number of degradation days, including data from the modern aged samples (*black symbols*) and the extrapolated values for the ancient samples (*blue symbols*). The three linear fits cross at approximately 212 artificial degradation days (see the text). Figure adapted from Ref. [39].

versus h (not reported in this work), which indicated that the water dynamics showed a minimum at ambient hydration ($h \sim 8\%$), confirming that this is the equilibrium condition for the samples made of pure cotton cellulose [39]. This means that the $h \leq 8\%$ paper behaves like a hydrophilic material, whereas the $h \geq 8\%$ paper shows hydrophobic behavior [39]. Indeed, for $h \leq 8\%$, cellulose attracts water molecules mainly through its hydroxyl groups. However, for $h \geq 8\%$, the hydroxyl groups of cellulose are no longer available for hydrogen bonding with water molecules. In such a case, the hydrophobic repulsion by glucopyranose ring moieties on the additional water molecules becomes important and water interactions with the degradation by-products are favored [39].

4 Conclusions

In this work, we report the results obtained on the degradation processes of ancient and modern aged and non-aged paper at different hydration levels by means of HR-MAS NMR spectroscopy. In samples diluted with D_2O, we found several by-products of the degradation processes. In particular, we identified (i) different carboxylic acids (both simple and complex) that were present in all the investigated samples and (ii) several amino acids (e.g., choline) that were characteristic only of the ancient samples and gave evidence of ancient production methods and/or geographical origins. Furthermore, we studied in detail the hydration and degradation processes by analyzing the NMR lineshapes and relaxation times. These investigations are very important for understanding how the cellulose fibers swell or how fast the kinetics of degradation are. Here, we report the best-fit and the corresponding parameters of the MAS NMR spectra of the hydrated samples by means of the pseudo-Voigt function expressed in Eq. (2). All parameters belonging to the Lorentzian component (corresponding to water) showed exponential-like behavior as a function of hydration. This was true for the both aged and non-aged samples characterized by different values of the exponential factor depending on the number of degradation days. We also report the data of the longitudinal relaxation time T_1 as a function of the hydration level h and of the number of degradation days. The HR-MAS technique that we used was able to discriminate between three different proton contributions to the whole dynamics belonging to free water, bound water, and cellulose. Our overall results indicate that hydration and degradation processes are interconnected and strictly dependent upon each other. In fact, the non-aged sample showed inert behavior upon the addition of water molecules and assumed properties similar to those in the bulk condition. However, the major presence of water accelerated the oxidative and hydrolytic mechanisms that progressively consumed the cellulose chains. In this way, different by-products with different complexities (carboxylic acids in particular) were increasingly produced. These by-products in turn influenced the properties of the water molecules present within the cellulose fibers. This characterization of the structural and dynamical properties of water molecules can provide a benchmark for determining the physical condition of cellulosic materials such as ancient paper. Moreover, this kind of knowledge can be applied for verification of the effectiveness of any restoration strategy.

Acknowledgements The authors acknowledge the Consiglio Nazionale delle Ricerche and the Istituto Centrale per il Restauro e la Conservazione del Patrimonio Archivistico e Librario (Roma, Italy) for their support. J. Łojewska is kindly acknowledged for providing the P2 samples. D.M.'s activity was carried out within the framework of the NANORESTART project, which has received funding from the European Union's Horizon 2020 research and innovation programme under grant agreement No. 646063.

References

1. F. Mallamace, C. Corsaro, D. Mallamace, S. Vasi, C. Vasi, P. Baglioni, S. V. Buldyrev, S. H. Chen, and H. E. Stanley, Energy landscape in protein folding and unfolding, *Proc. Natl. Acad. Sci. USA* 113(12), 3159 (2016)
2. F. Mallamace, C. Corsaro, D. Mallamace, S. Vasi, C. Vasi, and G. Dugo, The role of water in protein's behavior: The two dynamical crossovers studied by NMR and FTIR techniques, *Comput. Struct. Biotechnol. J.* 13, 33 (2015)
3. F. Mallamace, P. Baglioni, C. Corsaro, S. H. Chen, D. Mallamace, C. Vasi, and H. E. Stanley, The influence of water on protein properties, *J. Chem. Phys.* 141(16), 165104 (2014)
4. F. Mallamace, C. Corsaro, D. Mallamace, S. Vasi, C. Vasi, H. E. Stanley, and S. H. Chen, Some thermodynamical aspects of protein hydration water, *J. Chem. Phys.* 142(21), 215103 (2015)
5. D. Klemm, B. Philipp, T. Heinze, U. Heinze, and W. Wagenknecht, Volume I: Fundamentals and Analytical Methods, Weinheim: WILEY-VCH Verlag GmbH, 1998
6. A. C. O'Sullivan, The structure slowly unravels, *Cellulose* 4(3), 173 (1997)
7. X. Qiu and S. Hu, "Smart" materials based on cellulose: A review of the preparations, properties, and applications, *Materials (Basel)* 6(3), 738 (2013)
8. J. Kim, Cellulose as a smart material, in: R. Malcolm Brown Jr. and Inder M. Saxena (Eds.), Cellulose: Molecular and Structural Biology, Springer Netherlands, 323–343 (2007)

9. M. Missori, C. Mondelli, M. De Spirito, C. Castellano, M. Bicchieri, R. Schweins, G. Arcovito, M. Papi, and A. C. Castellano, Modifications of the mesoscopic structure of cellulose in paper degradation, *Phys. Rev. Lett.* 97(23), 238001 (2006)
10. M. De Spirito, M. Missori, M. Papi, G. Maulucci, J. Teixeria, C. Castellano, and G. Arcovito, Modifications in solvent clusters embedded along the fibers of a cellulose polymer network cause paper degradation, *Phys. Rev. E* 77(4), 041801 (2008)
11. K. L. Kato and R. E. Cameron, A review of the relationship between thermally-accelerated ageing of paper and hornification, *Cellulose* 6(1), 23 (1999)
12. G. Banik and I. Brückle, Structure and properties of dry and wet paper, in: Paper and Water: A Guide for Conservators, Amsterdam: Elsevier, 81–105 (2011)
13. L. Teodonio, M. Missori, D. Pawcenis, J. Lojewska, and F. Valle, Nanoscale analysis of degradation processes of cellulose fibers, *Micron* 91, 75 (2016)
14. C. Corsaro, D. Mallamace, J. Lojewska, F. Mallamace, L. Pietronero, and M. Missori, Molecular degradation of ancient documents revealed by ^{1}H HR-MAS NMR spectroscopy, *Sci. Rep.* 3, 2896 (2013)
15. D. Hunter, Papermaking: The History and Technique of an Ancient Craft, New York: Dover Publications, 1978
16. D. Capitani, A. L. Segre, D. Attanasio, B. Blicharska, B. Focher, and G. Capretti, ^{1}H NMR relaxation study of paper as a system of cellulose and water, *Tappi J.* 79, 113 (1996)
17. D. Capitani, N. Proietti, F. Ziarelli, and A. L. Segre, NMR study of water-filled pores in one of the most widely used polymeric material: The paper, *Macromolecules* 35(14), 5536 (2002)
18. C. Federici, P. Mufanò, and M. S. Storace, Ancient paper and its NMR characterization, *Sci. Technol. Cult. Herit.* 5, 37 (1996)
19. M. Missori, M. Righini, and A. L. Dupont, Gelatine sizing and discoloration: A comparative study of optical spectra obtained from ancient and artificially aged modern papers, *Opt. Commun.* 263(2), 289 (2006)
20. J. Kolar, Mechanism of autoxidative degradation of cellulose, *Restaurator (Copenh.)* 18(4), 163 (1997)
21. S. Zervos, Natural and accelerated ageing of cellulose and paper: A literature review, in: A. Lejeune and T. Deprez (Eds.), Cellulose: Structure and Properties, Derivatives and Industrial Uses, Nova Publishing, 155–203 (2010)
22. T. jewski, P. Miskowiec, M. Missori, A. Lubanska, L. M. Proniewicz, and J. Lojewska, FTIR and UV/vis as methods for evaluation of oxidative degradation of model paper: DFT approach for carbonyl vibrations, *Carbohydr. Polym.* 82(2), 370 (2010)
23. A. Mosca Conte, A. Knapik, J. Bagniuk, R. Del Sole, J. Lojewska, and M. Missori, Role of cellulose oxidation in the yellowing of ancient paper, *Phys. Rev. Lett.* 108(15), 158301 (2012)
24. T. jewski, T. Sawoszczuk, J. M. Lagan, K. Zieba, A. Baranski, and J. Lojewska, Furfural as a marker of cellulose degradation. A quantitative approach, *Appl. Phys. A* 100(3), 873 (2010)
25. Z. Souguir, A. L. Dupont, and E. R. de la Rie, Formation of brown lines in paper: Characterization of cellulose degradation at the wet-dry interface, *Biomacromolecules* 9(9), 2546 (2008)
26. A. L. Dupont, A. Seemann, and B. Lavédrine, Capillary electrophoresis with electrospray ionization-mass spectrometry for the characterization of degradation products in aged papers, *Talanta* 89, 301 (2012)
27. S. Belton, NMR studies of hydration in low water content biopolymer systems, *Magn. Reson. Chem.* 49, S127 (2011)
28. C. Violante, L. Teodonio, A. Mosca Conte, O. Pulci, I. Kupchak, and M. Missori, An ab-initio approach to cultural heritage: The case of ancient paper degradation, *Phys. Status Solidi B* 252(1), 112 (2015)
29. M. Missori, Optical spectroscopy of ancient paper and textiles, *Nuovo Cimento C* 39, 293 (2016)
30. M. Missori, O. Pulci, L. Teodonio, C. Violante, I. Kupchak, J. Bagniuk, J. jewska, and A. M. Conte, Optical response of strongly absorbing inhomogeneous materials: Application to paper degradation, *Phys. Rev. B* 89(5), 054201 (2014)
31. A. Mosca Conte, O. Pulci, M. C. Misiti, J. Lojewska, L. Teodonio, C. Violante, and M. Missori, Visual degradation in Leonardo da Vinci's iconic self-portrait: A nanoscale study, *Appl. Phys. Lett.* 104(22), 224101 (2014)
32. T. Rosenau, A. Potthast, K. Krainz, Y. Yoneda, T. Dietz, Z. P.I. Shields, and A. D. French, Chromophores in cellulosic, VI: First isolation and identification of residuals chromophores from aged cotton linters, *Cellulose* 18(6), 1623 (2011)
33. A. Abragam, The Principles of Nuclear Magnetism, London: Oxford University Press, 1961
34. S. Moestue, B. Sitter, T. Frost Bathen, M. B. Tessem, and I. S. Gribbestad, HR MAS MR spectroscopy in metabolic characterization of cancer, *Curr. Top. Med. Chem.* 11(1), 2 (2011)
35. A. Torre, F. Trischitta, C. Corsaro, D. Mallamace, and C. Faggio, Digestive cells from Mytilus galloprovincialis show a partial regulatory volume decrease following acute hypotonic stress through mechanisms involving inorganic ions, *Cell Biochem. Funct.* 31(6), 489 (2013)
36. O. Beckonert, M. Coen, H. C. Keun, Y. Wang, T. M. D. Ebbels, E. Holmes, J. C. Lindon, and J. K. Nicholson, High-resolution magic-anglespinning NMR spectroscopy for metabolic profiling of intact tissues, *Nat. Protoc.* 5(6), 1019 (2010)
37. C. Corsaro, D. Mallamace, S. Vasi, V. Ferrantelli, G. Dugo, and N. Cicero, ^{1}H HR-MAS NMR spectroscopy and the metabolite determination of typical foods in mediterranean diet, *J. Anal. Methods Chem.* 2015, 1 (2015)

38. N. Cicero, C. Corsaro, A. Salvo, S. Vasi, S. V. Giofré, V. Ferrantelli, V. Di Stefano, D. Mallamace, and G. Dugo, The metabolic profile of lemon juice by proton HR-MAS NMR: The case of the PGI Interdonato Lemon of Messina, *Nat. Prod. Res.* 29(20), 1894 (2015)
39. C. Corsaro, D. Mallamace, S. Vasi, L. Pietronero, F. Mallamace, and M. Missori, The role of water in the degradation process of paper using ^{1}H HR-MAS NMR spectroscopy, *Phys. Chem. Chem. Phys.* 18(48), 33335 (2016)
40. D. Mallamace, S. Vasi, M. Missori, and C. Corsaro, New insight into hydration and aging mechanisms of paper by the line shape analysis of proton NMR spectra, *Il Nuovo Cimento C* 39, 309 (2016)
41. J. H. Chen and S. Singer, High-resolution magic-angle-spinning NMR spectroscopy, in: J. C. Lindon, J. K. Nickolson, and E. Holmes (Eds.), The Handbook of Metabolonomics and Metabolomics, New York: Elsevier, 113–147 (2007)
42. J. C. Lindon, E. Holmes, and J. K. Nicholson, Metabolonomics in pharmaceutical R&D, *FEBS J.* 274(5), 1140 (2007)
43. E. R. Andrew, A. Bradbury, and R. G. Eades, Removal of bipolar broadening of nuclear magnetic resonance spectra of solids by specimen rotation, *Nature* 183(4678), 1802 (1959)
44. B. Blicharska and M. Kluza, NMR relaxation in cellulose pulp, *Colloids Surf. A Physicochem. Eng. Asp.* 115, 137 (1996)
45. D. Topgaard and O. Söderman, Changes of cellulose fiber wall structure during drying investigated using NMR self-diffusion and relaxation experiments, *Cellulose* 9(2), 139 (2002)
46. N. Matubayasi, C. Wakai, and M. Nakahara, NMR study of water structure in super- and subcritical conditions, *Phys. Rev. Lett.* 78(13), 2573 (1997)
47. K. Modig, B. G. Pfrommer, and B. Halle, Temperature-dependent hydrogen-bond geometry in liquid water, *Phys. Rev. Lett.* 90(7), 075502 (2003)
48. D. Sebastiani and M. Parrinello, Ab-initio study of NMR chemical shifts of water under normal and supercritical conditions, *ChemPhysChem* 3(8), 675 (2002)
49. F. Mallamace, C. Corsaro, M. Broccio, C. Branca, N. Gonzalez-Segredo, J. Spooren, S.H. Chen, and H. E. Stanley, NMR evidence of a sharp change in a measure of local order in deeply supercooled confined water, *Proc. Natl. Acad. Sci. USA* 105(35), 12725 (2008)
50. C. Corsaro, J. Spooren, C. Branca, N. Leone, M. Broccio, C. Kim, S. H. Chen, H. E. Stanley, and F. Mallamace, Clustering dynamics in water/methanol mixtures: A nuclear magnetic resonance study at 205 K $< T <$ 295 K, *J. Phys. Chem. B* 112(34), 10449 (2008)
51. M. F. Froix and R. Nelson, The interaction of water with cellulose from nuclear magnetic resonance relaxation times, *Macromolecules* 8(6), 726 (1975)
52. D. Majolino, C. Corsaro, V. Crupi, V. Venuti, and U. Wanderlingh, Water diffusion in nanoporous glass: An NMR study at different hydration levels, *J. Phys. Chem. B* 112(13), 3927 (2008)
53. M. Paci, C. Federici, D. Capitani, N. Perenze, and A. L. Segre, NMR study of paper, *Carbohydr. Polym.* 26(4), 289 (1995)
54. S. Hayashi and E. Akiba, Nuclear spin-lattice relaxation mechanisms in kaolinite confirmed by magic-angle spinning, *Solid State Nucl. Magn. Reson.* 4(6), 331 (1995)
55. E. Scarpellini, M. Ortolani, A. Nucara, L. Baldassarre, M. Missori, R. Fastampa, and R. Caminiti, Stabilization of the tensile strength of aged cellulose paper by Cholinium-Amino acid ionic liquid treatment, *J. Phys. Chem. C* 120(42), 24088 (2016)